CMIP5 Projected Changes in the Annual Cycle of Precipitation in Monsoon Regions

ANJI SETH *

Department of Geography, University of Connecticut, Storrs, Connecticut

SARA A. RAUSCHER

Los Alamos National Laboratory, Los Alamos, New Mexico

MICHELA BIASUTTI, ALESSANDRA GIANNINI AND SUZANA J. CAMARGO

Columbia University, Palisades, New York

MAISA ROJAS

University of Chile, Santiago, Chile

* *Corresponding author address:* Anji Seth, Department of Geography, University of Connecticut, U-4148 215 Glenbrook Rd., Storrs, CT 06269.

E-mail: anji.seth@uconn.edu

ABSTRACT

While projected total precipitation changes in monsoon regions are uncertain, twenty first century climate model projections show an amplification of the annual cycle in tropical precipitation with increased strength in both wet and dry seasons. New analysis of World Climate Research Program (WCRP) Coupled Model Intercomparison Project phase 5 (CMIP5) data are mostly consistent with those from CMIP3, and indicate reductions in early and increases in late summer precipitation in multi-model ensemble 21^st century climate projections for monsoon regions.The precipitation changes in the annual cycle are linked with two competing mechanisms in a warmer world. In winter, drier conditions prevail due to warmer upper troposphere, increased stability (especially over land), and increased moisture divergence associated with the descending branch of the Hadley circulation (the remote effect). During the summer wet season, enhanced evaporation and decreased stability due to increased surface moist static energy (MSE) lead to increased precipitation (the local effect). However, during spring and early summer, even after tropospheric stability decreases due to an increase in low-level MSE, precipitation reductions continue for a short period. Examination of the moisture budget through the annual cycle shows that increased divergence and reduced evaporation characterize the transition from dry to wet seasons. Surface moisture, which is essential for the local mechanism to engage, is therefore lacking at the end of a warmer and drier dry season. Thus both remote and local mechanisms act to create an enhanced early summer convective barrier which helps to reduce early season rainfall; however, once sufficient moisture is imported, decreases in tropospheric stability result in precipitation increases.

These changes are particularly apparent in the American and African monsoons. Important exceptions are the Asian and Southeast Asian monsoon regions, where evaporation is abundant through the dry season, divergence is unchanged, and precipitation is does not decrease in spring and early summer. These regionally variable responses and an overall weaker northern hemisphere response compared to CMIP3 may be due to factors other than

greenhouse gas forcing in the RCP8.5 scenario. Nonetheless, while the models continue to exhibit substantial biases in tropical precipitation, there is more model agreement in the annual cycle changes than in annual or warm season means. These results further demonstrate that the role of local evaporation and boundary layer moisture in the land-based monsoon regions is critical in determining the regional transition season response. Changes in the global monsoon precipitation have been difficult to evaluate both in observations and projections. As described in our results, viewing monsoons from their inherent ties to the annual cycle could help to fingerprint changes as they evolve.

1. Introduction

This analysis focuses on 21st century projections of the annual cycle of tropical precipitation in monsoon regions (e.g. Wang and Ding 2006; Trenberth et al. 2000). Seasonally wet/dry monsoons result from directional shifts in winds and moisture transport due to the longer response time of oceans versus land to the annual cycle of solar heating (Chao and Chen 2001; Webster et al. 1998). The global monsoon has been defined as a seasonally varying, persistent overturning of the atmosphere throughout the global tropics and subtropics with the annual cycle of solar heating as its primary driver. Regional monsoons are embedded in this large scale overturning and connections between regions result from the requirement of mass conservation (Trenberth et al. 2000). There are ongoing efforts to examine coherent responses of the global monsoon to internal and external forcings which evolve on interannual (ENSO) (Wang et al. 2012) and longer (greenhouse gases) time scales in recent observations and climate model projections (Fasullo 2012).

Under radiative forcing scenarios dominated by increasing greenhouse gas concentrations, land-sea thermal contrasts are expected to increase. The increase is in part due to differences in thermal inertia between land and ocean, but largely because oceans divert more of the anomalous incoming energy into latent heat rather than increasing surface temperature (Sutton et al. 2007). Where moisture is abundant (i.e., over oceans) warmer surface temperatures lead to increased evaporation and robust increases in atmospheric water vapor due to the nonlinear Clausius-Clapeyron relationship, which are associated with weakening of the tropical (Hadley, Walker and monsoon) circulations (Held and Soden 2006).

Despite the weakening of tropical circulations, the World Climate Research Programme (WCRP) 3rd Coupled Model Intercomparison Project (CMIP3) multi-model climate projections suggested a tendency towards increased monsoon precipitation and increased low-level moisture convergence (Christensen et al. 2007). Precipitation increases have been documented in CMIP3 projections for Australia (Meehl et al. 2007) and South Asia (Douville et al. 2000). In South Asia a 5-25% increase in precipitation was found in the models that best represented the interannual variability and teleconnections associated with the monsoon (Annamalai et al. 2007). However, the North American monsoon region is expected to become drier in the annual mean (Seager et al. 2007), and much uncertainty exists for the future of the West African and South American monsoons (e.g. Giannini et al. 2008; Vera et al. 2006). The response of global monsoons to greenhouse warming is complicated by a number of factors, including the dynamical weakening of the tropical circulation (Tanaka et al. 2005; Vecchi and Soden 2007), related changes in the tropical tropospheric stability (Chou et al. 2001; Neelin et al. 2003), and the regional effects of aerosols and black carbon (Lau et al. 2006; Meehl et al. 2008).

Most previous studies have focused on the fully established wet and dry seasons (Dec-Feb, Jun-Aug). However, studies that examine the full annual cycle indicate a redistribution of precipitation within the rainy season. For example, the South American and West African monsoons both exhibit drying in spring and increased precipitation during summer in projections (Seth et al. 2009; Biasutti and Sobel 2009; Biasutti et al. 2009). Despite the disagreement among climate models regarding projections of annual or warm season mean Sahel precipitation in the 21st century (e.g. Giannini et al. 2008), there is near consensus regarding a weakening of early and strengthening of late season rainfall (Biasutti and Sobel 2009). Models indicate a similar reduction in spring and an increase in summer precipitation in the core region of the South American monsoon, which is associated with insufficient low level moisture convergence in spring and a substantial increase in convergence during summer (Seth et al. 2009).

Our study of monsoons based on CMIP3 data found a redistribution of precipitation from early to late summer in five of seven monsoon regions globally (Seth et al. 2011, hereafter, SRRGC). The analysis of twentieth century (20C) and SRES A2 scenario experiments employed a moist static energy (MSE) framework, which exploits the role of evaporation in both energy and water budgets (Neelin and Held 1987). Based on Giannini (2010), two competing mechanisms were examined, involving the differing responses of simulated precipitation to greenhouse gas forcing: *remote* (or top down) and *local* (or bottom up). A schematic of these mechanisms is provided in Fig. 1. In the *remote* mechanism, large scale tropospheric warming controls vertical stability in the global tropics (Sobel et al. 2002; Chiang and Sobel 2002), and reduces continental precipitation in those regions that cannot meet the increasing demand for near-surface moist static energy (Chou et al. 2001; Neelin et al. 2003). In this case, the precipitation reduction is reinforced by a consequent reduction in evaporation due to decreased precipitation recycling. In the second, *local* mechanism, the land surface response to anthropogenically enhanced terrestrial radiative forcing dominates. Where surface moisture is sufficient, increased evaporation leads to near-surface increases in moist static energy, instability, and precipitation. The increase in precipitation is then reinforced by enhanced moisture convergence. Where moisture is insufficient, increased terrestrial radiation is balanced by increased sensible heat flux. In our CMIP3 analysis, the *remote* mechanism dominates during the dry season and the *local* mechanism dominates during the rainy season. During the transition from dry to wet (i.e., in spring) the our results suggested that insufficient moisture availability at the end of an intensified dry season would favor an extension of the top down mechanism and delay the hand off to bottom up destabilization, resulting in diminished early season rainfall. A similar mechanism has been suggested, to explain CMIP3 projected mean summer precipitation changes in monsoon regions (Fasullo 2012). In this study increased low level moisture convergence was required as surface temperatures increase and near surface relative humidity decreases over land, which is consistent with their analysis of recent observations.

The above mechanisms have focused on understanding the land response in monsoon regions. Meanwhile, possible causes for the changes in the global tropical annual cycle are also being investigated. Dwyer et al. (2012) have shown that a projected delay in high latitude SST, due to reductions in sea ice, is not likely to be a cause of the changes in the tropical annual cycle. However, increases in the amplitude of low latitude SST could play a role in delaying monsoon precipitation (Dwyer, 2012, personal communication). An alternative possibility is that a poleward shift in mid-latitude storm tracks is largely responsible for the springtime weakening of rainfall in monsoon regions (Scheff and Frierson 2012a,b).

In the present study a new suite of experiments from the WCRP 5th Coupled Model Intercomparison Project (CMIP5) archive (Taylor et al. 2011) are analyzed to further explore the response of precipitation in monsoon regions to radiative forcings in the 21st century. The analysis is extended beyond that of SRRGC to evaluate the role of changes in the divergence of moisture fluxes in delaying the development of the *local* mechanism in spring. This analysis is performed through the annual cycle, thus permitting a view of both transition seasons. We show that, despite model uncertainties in annual precipitation, a shift in the annual cycle is continues to be discernable in the CMIP5 projections and is part of a global response to greenhouse forcing. However, there are notable changes from the CMIP3 results. The remainder of this paper is structured as follows: the coupled climate models, experiments and observations employed in this research are described in Section 2. In Section 3, results are presented from the CMIP5 database for present day and future periods using the Historical and RCP8.5 experiments. Discussion of results and analysis of additional experiments is provided in Section 4, with a summary and conclusions in Section 5.

2. Methods

This analysis employs multi-model ensemble experiments from the WCRP CMIP5 dataset (Taylor et al. 2011). Historical simulations (hereafter, Hist) are analyzed and compared with observed estimates from the Climate Prediction Center (CPC) Merged Analysis of Precipitation (CMAP) version 2 (Xie and Arkin 1996), which employes satellite and gauge data in a globally gridded product for the recent period (1981-2005).

The 21st century experiments in CMIP5 are based on representative concentration pathways (RCP's) (van Vuuren et al. 2011). We analyze the higher concentration scenario in which the net radiative forcing in the year 2100 is 8.5 W/m^2 and focus on 30-year periods for the historical (Hist, 1971-2000) and late 21st century (RCP8.5, 2071-2100). Note that the RCP8.5 scenario yields a larger global mean temperature response (+0.7 ^{o}C) compared to the SRES A2 scenario CMIP3 results (Rogelj et al. 2012). In addition, the CMIP5 models have different implementations of the effects of short-lived radiatively active trace gases and aerosols (Lamarque et al. 2011), which further complicate comparisons between CMIP3 and CMIP5 results. Seventeen models, identified in Table 1, comprise the ensemble for which monthly precipitation, moist static energy, divergence and evaporation are examined for the Hist and RCP8.5 experiments. In addition, the preindustrial Control (piCont) and the transient 1% CO2 (1%CO2), are examined in order to isolate and simplify the climate response to greenhouse gas radiative forcing. Data from the piCont and 1%CO2 experiments are limited to an eleven-model subset (identified by stars in Table 1).

While comparison with the CMIP3 results of SRRGC cannot be made directly due to the many differences in the models and scenarios, the monsoon regions are defined similarly for some degree of consistency, as follows: North America (NAM, 115-102.5W, 20-35N), South America (SAM, 60-40W, 10-25S), West Africa (WAf, 10W-10E, 10-25N), South Africa (SAf, 20-40E, 10-25S), South Asia (SAsia, 65-85E, 10-25N), Southeast Asia (SEA, 100-120E, 10-25N), and Australia (Aus, 130-150E, 10-25S). These regions are identified as boxes on the map in Fig. 2. Precipitation results are shown as percent differences to allow for comparison with SRRGC where possible. However, in the moisture budget discussion all variables are shown in mm/day. All model data have been regridded to the 64 x 128 (T42) resolution.

3. Results

In this section the following questions are posed: (1) Do the CMIP5 models show a response in the annual cycle similar to CMIP3? Given the stronger radiative forcing in RCP8.5 compared to that in SRES A2, the expectation would be for a similar, if not stronger, response. (2) How do the CMIP5 models simulate the annual cycle in the monsoon regions for the recent observed record? (3) If the CMIP5 models show a redistribution from early to late summer, is the response embedded in a coherent global scale change in the annual cycle? (4) Why do the regional monsoons respond as they do? Does the mechanism suggested by SRRGC hold in these new results, and what role is played by moisture transport?

The projected regional precipitation changes are presented in Fig. 2 which shows a map of the early summer (June/November) ensemble mean percent differences in the northern/southern hemisphere. Also shown are precipitation differences (mm/day, masked for areas with < 0.5 mm/day) in bar plots for each region, with individual model responses shown by month in the annual cycle. This map illustrates the global scale of the subtropical spring response, with decreases in rainfall projected throughout the subtropics (10-30^o poleward of the equator). Also noticeable are the different responses of the Asian monsoons compared to the monsoons in the Americas and Africa. The bar plots provide an indication of the agreement among the models regarding the sign and magnitude of precipitation change by month. For the American and African monsoons, while the average of the rainy season may show little or no change in precipitation (and model disagreement on the sign of the change), the annual cycle presents a stronger model agreement in reduction of early and increase in late season rainfall. The models also agree regarding the projected precipitation increases in the South and Southeast Asian monsoons. The Australian monsoon precipitation response remains uncertain through most of the annual cycle.

Evaluation of simulated annual cycle

Because the CMIP5 dataset is new, the multi-model ensemble precipitation annual cycle is briefly evaluated. The observed (CMAP) annual cycle is shown in Fig. 3 (black contours with thicker contours beginning at 5 mm/day), as a latitude vs time Hoevmoeller plot of with the zonal mean averaged precipitation for the longitudes in each monsoon region. The latitude axis provides a view of the poleward migration of rainfall during the warm season. The monsoons in the northern hemisphere exhibit peak rainfall and poleward extension in

July and August, and those in the southern hemisphere during January and February. The multi-model ensemble mean bias (difference from CMAP) is shown in color, and it is clear that the CMIP5 suite of models still has problems representing the monsoon rainfall: the models are drier than observed in the early rainy seasons of South America and South Asia and wetter in the late rainy season. Through much of the rainy seasons in Southeast Asia and Australia equatorward of 20^o latitude they are also too dry. The precipitation in West Africa is overestimated, except in July and August on the northern margin of the monsoon, where the models exhibit a modest dry bias. In North America and South Africa the models overestimate rainfall. Although spring dry biases are evident in several regions, the structure of the errors by latitude and month appears to be unique to each region without consistency between regions. Results from analysis of projections will be considered in the context of these model errors in Section 4.

Global scale changes in the tropical annual cycle

In the CMIP3 projections of future climate change under a high greenhouse gas forcing scenario (A2), a robust large-scale signal emerged in tropical and subtropical precipitation. Summer hemisphere wet seasons and winter hemisphere dry seasons simultaneously strengthened, creating an asymmetric inter-hemispheric response(Tan et al. 2008), with impacts in various characteristics of the summer tropical climate response (Sobel and Camargo 2010). In the global monsoon, this shift was visible as an extension of the dry season into spring, and an enhancement of late summer precipitation (see Fig. 2(a,b) in SRRGC). Here we see a similar response in the CMIP5 models, as shown in the top panels in Fig. 4 which present the annual cycle of zonal mean precipitation in the tropics (land and ocean) for the Historical experiments and changes in the RCP8.5 scenario. The global precipitation annual cycle (black contours, with thicker contours beginning at 5 mm/day) shows the tropical rainfall band migrating poleward in the summer hemisphere (DJF, southern and JJA, northern). The intensification of both wet and dry seasons is apparent in the projected changes (colors).

During the transition from dry to wet season, there is a reduction of precipitation (4a). This suggests that in the global monsoon, there is a redistribution of precipitation from early to late rainy season.

If we consider land only (4b), the precipitation reduction is comparatively weaker in its extension into the northern summer months, but the opposite is true for the southern hemisphere, which shows a stronger response over land compared to the global mean. This suggests that the southern hemisphere continental monsoon regions should exhibit a stronger early season drying, while those in the northern hemisphere may not. Nonetheless, the late rainy seasons (Feb–Mar, Aug–Sep) show clear strengthening of summer rainfall in both hemispheres. Compared to CMIP3, the northern hemisphere response in CMIP5 over land is weaker, as in CMIP3 both the northern and southern hemispheres displayed a more noticeable extension of the dry season in the land-only averages compared to global averages. This weaker northern hemisphere response will be examined further in Section 4 through the use of the CO2-only experiments.

The *remote* and *local* mechanisms are examined using changes in the vertical gradient of moist static energy, defined as $MSE = DSE + Lq$. The dry static energy is defined as $DSE = c_pT + gZ$, where c_p is the specific heat at constant pressure, T is the layer temperature, g is gravity, Z is the geopotential height, L is the latent heat of evaporation, and q is the specific humidity. Recall that the remote mechanism is related to increased stability that results from a warmer tropical troposphere. The gross stability of the tropical tropospheric is the difference between MSE in the poleward flow at upper levels and the low-level equatorward flow (Held 2001). Thus, as a measure of the free tropospheric stability, we examine changes in the vertical gradient of moist static energy, $vMSE$, which is defined $vMSE = MSE_{200} - MSE_{850}$.

Fig. 4 (c,d) presents the annual cycle of zonal mean $vMSE$ (4c) and for land only (**??**), where positive (negative) changes in vMSE indicate greater stability (instability), which would tend to inhibit (enhance) precipitation in future projections. Precipitation % differences (RCP8.5 - Hist) are also shown in Fig. 4 (c,d) as black contours. Despite future projected increases in surface temperatures and humidity, changes in tropospheric stability are not consistent throughout the year in the subtropics. In winter, the $vMSE$ increases, indicating greater stability to convection, and in summer it becomes more negative (*i.e.*, less stable). Fig. 4(d) also shows that during the spring transition from dry to wet seasons (Aug-Oct and Mar-May), the increase in $vMSE$ persists, indicating increased stability to convection over land. Therefore, the projected springtime drying is controlled at least in part by the *remote* (top down) mechanism.

If we examine Fig. 4(d) closely, the wintertime decrease in precipitation continues into November (southern hemisphere spring), even after $vMSE$ indicates a transition from a more stable to a less stable troposphere. The extension of the drying into early summer was examined in SRRGC by separating $vMSE$ into its temperature and moisture terms and was shown that the early summer increase in low level moist static energy resulted from the temperature term. Only after the moisture term increased in early summer did the precipitation change reverse from drier to wetter conditions. In the CMIP5 simulations, similar changes in temperature and moisture terms occur over the southern hemisphere (not shown). However, again the northern hemisphere response in the CMIP5 models differs from CMIP3. The lag between the decrease in $vMSE$ and the increase in precipitation in the northern hemisphere is smaller or even arguably absent in CMIP5 compared to CMIP3. We will investigate further the northern hemisphere reduction in the global signal of springtime drying over land by examining additional experiments in Section 4. The next question is: what is the regional response in each monsoon?

Annual cycle changes in monsoon regions

To analyze the regional monsoon responses, the CMIP5 ensemble mean changes in the zonal mean annual cycles of precipitation (averaged over longitudes of each monsoon region) are shown in Fig. 5 (c-i, see Methods for region definitions which are shown in Fig. 2). Here the regional precipitation is masked for land only grid points and the simulated climatology (black contours with thicker lines beginning at 5 mm/day) shows the poleward migration of precipitation during the warm season (JJA, northern and DJF, southern). An intensification of the dry season is seen in all of the regional monsoons. Early summer decreases and late summer increases in precipitation are evident in the American and African monsoon regions in both hemispheres. However, South and Southeast Asia show little change during spring and much of the rainy seasons. Compared with CMIP3 (SRRGC), the CMIP5 results indicate stronger responses in the Americas and Africa (expected due to the stronger radiative forcing in the RCP8.5 scenario) but a weaker response in Southeast Asia.

The remote and local mechanisms are further investigated for each region, using our measure of changes in vertical stability, $vMSE$. Fig. 6 shows projected changes in the zonal mean annual cycle of $vMSE$, with precipitation changes given in mm/day (black contours). All monsoon regions exhibit increased vertical stability (remote mechanism) during the dry season and increased instability (local mechanism) during the rainy season (not shown). In addition, the spring drying extends beyond the reversal of $vMSE$ to an increased instability in the transition from dry to wet seasons. Previous results showed that where the precipitation decreases continue beyond the transition to a decreased stability (according to the $vMSE$ measure) the low level increases in MSE were due largely to increases in temperature rather than moisture. At the end of the dry season, local evaporation is likely to be less important than atmospheric moisture transport into the region. Because the transition from dry to wet seasons depends upon atmospheric moisture transport, our next step is to examine projected changes in the divergence of moisture fluxes.

Evaluation of moisture budget

In monsoon regions, the transition from the dry to the wet season occurs in three phases. First, where surface moisture is available, available potential energy increases locally due to increasing latent heat fluxes (initiation). Second, a transition in the large-scale circulation leads to net moisture convergence (development). Finally, in the mature onset phase, an upper-tropospheric anti-cyclonic circulation continues to spin up until it reaches its full strength (Li and Fu 2004). The monsoon can therefore be delayed due to lower latent heat fluxes associated with negative springtime soil moisture anomalies (Collini et al. 2008; Small 2001). Once the rainy season begins, the local land surface influence becomes less important (Li and Fu 2004), although land wetness anomalies can also influence rainfall during the monsoon season (Taylor et al. 2010; Grimm et al. 2007). To investigate changes in the atmospheric moisture budget, we examine its components: precipitation, moisture flux divergence, and evaporation, all in units of mm/day, in the global tropics as well as in the regional monsoons.

Ensemble mean changes in the global zonal mean annual cycle of moisture flux divergence are shown in Fig. 7(c,d) with the precipitation (now in mm/day for comparison with divergence (7a,b) and evaporation (7e,f). The simulated 1981-2005 climatologies (black contours) are also given for each variable and illustrate the model seasonal evolution of moisture in the global monsoon. The tropical rainfall band migrates seasonally, as well as the moisture convergence (dashed lines in 7c,d) which follows the maximum in solar heating. The global zonal mean evaporation is greater than 3 mm/day with a weak annual cycle, however, over land evaporation with values greater than 3 mm/day is confined to the migrating band of tropical rainfall and convergence, *i.e.*, the global monsoon.

Comparing precipitation to moisture divergence changes reveals that globally the projections indicate increased convergence in regions of climatological convergence and increased divergence in regions of climatological divergence, consistent with many earlier results (e.g., Chou and Neelin 2004). Over southern hemisphere land areas, increased divergence and decreased evaporation (7d,f) are coincident with spring and early summer (Oct/Nov) precipitation decreases (7b). Northern hemisphere changes are less noticeable and not significant in the CMIP5 results.

Figs. 8, 9 and 10 show the changes in moisture flux divergence, evaporation and near surface relative humidity in the individual monsoon regions, to be compared with precipitation changes in Fig. 5. The simulated climatological values of each variable are given as black contours. In addition, the maps in Figs. 11 and 12 show the early (June in northern and November in southern hemispheres) and late (September, northern and February, southern hemispheres) summer changes in precipitation, moisture flux divergence and evaporation. Here we discuss each region and follow by summarizing the common responses.

In North America precipitation decreases year round, except for a short period of projected increase in the late rainy season (Sep–Oct). The maxima in precipitation decreases (increases) are associated with maxima in moisture flux divergence increases (decreases), and there is a weaker increase in convergence in April and May that does not yield an increase in rainfall. Evaporation rates are unchanged after the rainy season (Aug–Dec) but then decrease through July with a maximum in April and May. This suggests that a reduction in moisture transport is important for the decrease in early summer precipitation, but decreased local evaporation plays a role throughout the spring and early summer by limiting the increase of boundary layer moisture, which can be seen as decreases in near surface relative humidity. Indeed, the map views in Figs. 11 and 12 show that in June evaporation plays a dominant role in reducing boundary layer humidity: evaporation is reduced throughout the region, while changes in moisture divergence are positive in the south and negative in the north. Thus, the North American monsoon is characterized by increased surface aridity, and requires additional moisture transport to meet an increased need for moisture in a warmer world.

The West African monsoon does not exhibit an intensified dry season, but projections do indicate a reduction in spring and early summer (May–Jul) with increased rainfall in late summer (Sep–Nov). The precipitation changes are closely associated with changes in moisture flux divergence where the maxima in divergence increases (decreases) are aligned with precipitation decreases (increases). Evaporation changes are negligible much of the year, but do show increases at the end of the rainy season (Sep–Nov) and a slight decrease in

April and May equatorward of 10^oN. The increased late season rainfall yields increases in near surface relative humidity (Sep–Nov), which then does not show much change from present until the early rainy season, when decreased convergence and rainfall result in lower relative humidity. The early season reduction of rainfall in the West African region, then, appears to result mostly from increased moisture flux divergence, with decreases in early season, with the local evaporation playing a small, generally less important role. This can be seen also in Fig. 11, while Fig. 12 shows the increase in late summer rainfall being associated with increases in both evaporation and moisture convergence.

In South America precipitation decreases are projected in both spring (Sep–Nov) and fall (Mar–Apr) equatorward of 25^oS. Coincident with these reductions are increases in rainfall between 25-35^oS, which have been shown to result from the poleward expansion of the South Atlantic subtropical anti-cyclone and the South Atlantic Convergence Zone (SACZ) (Seth et al. 2011). During the peak rainy season (Dec–Feb) rainfall increases in the CMIP5 projections. The rainfall changes are again closely aligned with changes in moisture flux divergence, however in spring, the reduction in moisture due to divergence is smaller than that due to reduced evaporation. Evaporation rates increase slightly towards the end of the rainy season, and then decline through the dry season with the maximum reduction occurring during the transition from dry to wet seasons (Sep–Nov). Near surface relative humidity is lower throughout the year, presumably due to warmer temperatures, with a sharp decrease in early rainy season (Sep–Nov) largely as a consequence of reduced evaporation with the moisture convergence having a smaller effect. The early season reduction in rainfall in South America results from a combination of reduced evaporation and reduced moisture transport into the region, while the early dry season reduction is largely due to increased moisture flux divergence. Figs. 11 and 12 are consistent with this picture and further suggest that evaporation and moisture transport changes contribute equally to drying in early summer. In late summer the local mechanism works effectively with increased evaporation and moisture convergence to yield excess rainfall.

The monsoon in Southern Africa responds similarly to that in South America in a number of ways. Precipitation decreases in spring (Sep–Nov) and increases in summer (Jan–Mar), as a consequence of changes in moisture flux divergence. Here too, reduced evaporation rates in spring (Sep–Nov) are comparable in magnitude to reduced moisture transport convergence (Fig. 11), which combine to amplify the reduction in boundary layer humidity as seen in the near surface relative humidity. Thus, the monsoon region in southern Africa is characterized by overall increased surface aridity, with insufficient local moisture at end of dry season, which requires moisture transport and additional convergence. Once this requirement is met increased convergence and rainfall occur (Fig. 12), but do not penetrate poleward of 20^{o}S, where drier conditions are apparent, with reduced evaporation through the annual cycle.

The annual cycle of rainfall in Southeast Asia shows small precipitation decreases during dry season into Mar–Apr, followed by increases through much of the rainy season (May–Nov). The rainfall increases can be explained in large part by coincident increases in moisture convergence. However, unlike the monsoon regions discussed above, in Southeast Asia, the evaporation increases dominate through the rainy season (Jun–Dec), with no decreases apparent in spring (see also Figs. 11 and 12). While near surface relative humidity does increase due to warmer temperatures, there are no sharp increases in spring resulting from a lack of local moisture availability or due to a strong reduction in moisture convergence. In this region, then, the local mechanism can operate as usual, without limitations on early season moisture availability. Overall, despite increased divergence in winter, there is ample local evaporation to moisten the boundary layer and initiate moisture convergence, which then increases to result in more rainfall and increased recycling due to increases in evaporation during the rainy season.

The South Asian monsoon has similarities to the Southeast Asia monsoon. Although increased divergence is strong during the dry season, precipitation changes are generally small, with only some reduction in rainfall (Jan–Apr). Increases in moisture convergence are seen beginning in July and extend through November, which can explain much of the increased rainfall seen during this period. Evaporation rates in the region are higher especially during the late rainy season, after rainfall has increased (Fig. 12), but they remain higher through much of the dry season. The lack of reduction in evaporation during winter and spring (Fig. 11) and no reduction in relative humidity both indicate that sufficient local moisture is available for the local mechanism to commence.

The Australian region is remarkable for the lack of overall changes projected in precipitation, moisture divergence and evaporation, though relative humidity near the surface increases due to warming temperatures. This lack of change is in contrast with the increases in rainfall projected from CMIP3 in the 4th Assessment Report (Meehl et al. 2007), and will be addressed further in the next section.

The four regions that exhibit the springtime drying (American and African monsoons) in the zonal mean annual cycles suggest that decreases in both moisture convergence and evaporation are responsible for the drying. Although the near surface relative humidity decreases through much of the year, the largest decreases are seen in spring, coincident with decreases in evaporation and convergence. Over South America and South Africa, the decreases in early summer evaporation and moisture convergence are similar in magnitude, suggesting that both play an important role in reducing moisture availability for the local mechanism to take effect. Over North America, the decrease in evaporation extends over the entire spring, while moisture convergence decreases in winter, increases briefly in spring, and then decreases in the early monsoon period. West Africa shows a stronger decrease in moisture convergence than evaporation. Interestingly, the two regions that do not show spring drying - Southeast Asia and South Asia - do show some decreases in moisture convergence in but no decreases in evaporation.

These results suggest that the effects of the remote mechanism - a reduction in winter precipitation - lead to an overall drier land surface and reduced evaporation in spring. Despite more energy being available to evaporate water in the future (and therefore feed back to precipitation via the local mechanism), the lack of surface moisture means that the local mechanism cannot be activated as it normally would to increase precipitation. This is also consistent with a reduction of near surface relative humidity due to increasing temperatures, with a maximum reduction in spring. Once the moisture transport into the region increases (i.e. moisture flux divergence decreases) the increase in low level moist static energy is sufficient for the local mechanism to initiate. Further, the increasing moisture transport and warmer temperatures result in greater rainfall and increased recycling through evaporation (e.g. Giannini 2010).

The results also suggest an important role for moisture availability during the transition from dry to wet seasons. In the regions where boundary layer (and surface) moisture remains abundant, there is no decrease in early season rainfall, yet those regions in which the boundary layer (and surface) "dries out" during winter, the transition to wet season requires a build-up of boundary layer moisture which relies on increased moisture transport.

4. Discussion Projections - 1%CO2

The CMIP5 results thus far suggest that the precipitation annual cycle response of the American and African monsoons is similar to those seen in CMIP3, with a redistribution of rainfall from early to late summer. However, the Southeast Asian monsoon shows a weaker response, i.e., less drying in early summer in CMIP5, and the global response in the Northern Hemisphere is also reduced. Thus, we return to the differences between CMIP5 and CMIP3 global tropical precipitation changes in northern hemisphere early summer.

Recall from the discussion of Fig. 4 (b,d) that the results of SRRGC indicated a stronger drying response over land than the global mean in both hemispheres. However, the present CMIP5 results do not show a stronger response over land in the northern hemisphere. Although the RCP8.5 scenario achieves a higher radiative forcing in the year 2100 (8.5 W/m^2) than did the SRES A2 scenario which was analyzed for CMIP3, the new scenario incorporates reductions in several aerosol species (including sulfate aerosols, black carbon and organic carbon) during the 21st century. The reductions are largest over Asia and Africa, and their effects can complicate the climatic response regionally (Lamarque et al. 2011; Villarini and Vecchi 2012). In addition, the A2 scenario employed in CMIP3 did not include as many aerosol species and the models simulated primarily their direct radiative effects. Therefore, in order to simplify and isolate the response to greenhouse gas forcing in the CMIP5 model suite we examine the 1%CO2 experiment using the piCont as the control for the 11-models available. In these idealized experiments with the CMIP5 models, if the northern hemisphere land response is similar to that seen in the CMIP3, then there is some basis to state that additional factors (beyond greenhouse gases) are playing a role in the reduced response in the RCP8.5 results.

We compare Fig. 13, which shows the global 1%CO2 minus PiCont precipitation and $vMSE$ to Fig. 4 (RCP8.5 minus Hist). Indeed, the idealized experiments results are similar to CMIP3, with a larger decrease in rainfall over land extending further into summer in the northern hemisphere as well as in the southern hemisphere. And as in CMIP3, the precipitation declines extend beyond the time at which the change in stability, given by $vMSE$, switches from more to less stable than present. Because these idealized CMIP5 experiments (with CO2 forcing only) show a response similar to that from CMIP3, we suggest that the "additional factors" incorporated in the RCP8.5 forcing are likely to be important in explaining the difference in the northern hemisphere response.

The regional monsoon precipitation changes in the idealized CMIP5 experiment are shown in Fig. 14. Compared with Fig. 5 the regional changes are generally consistent, but with some differences. There is a greater early summer drying and a reduced late season precipitation increase in the Southeast Asian and West African regions in this simplified greenhouse gas experiment. At the same time the South Asian monsoon shows increased rainfall earlier (in June rather than July) in the idealized case compared with the RCP8.5 scenario.

The CMIP5 aerosol forcing reductions during the 21st century are larger than those employed in CMIP3 yielding fewer aerosol species in 2100, especially over Asia and Africa, where they are relatively abundant in present day. According to recent observational and modeling studies, while monsoon precipitation responses to various aerosol species can be complex, the expectation is for an increase in monsoon precipitation given a reduction in aerosol counts. If this is indeed the case, the CMIP5 results, which show increased precipitation in spring in the Southeast Asian and African monsoons are consistent with the changes in aerosol forcing from CMIP3 (Lamarque et al. 2011; Turner and Annamalai 2012).

These results further suggest that monsoon region annual cycle responses are related to the greenhouse gas forcing, and reductions in this response are likely due to the complex effects of additional factors in the RCP8.5 scenario in three of the four northern monsoons and hence, the global signal. On the other hand, rainfall anomalies in Australia do not conform to the expected pattern of early season decrease and late season increase, a result that stresses how regional and local-scale rainfall changes continue to be uncertain.

5. Conclusions

Twenty-first century projections of precipitation in a number of monsoon regions have been plagued by uncertainty due to model disagreement on even the direction of change (Giannini et al. 2008; Turner and Annamalai 2012; Vera et al. 2006). Yet several recent studies have suggested that coherent shifts can be seen within the annual cycle, which are not represented in annual or warm season averages (Biasutti and Sobel 2009; Seth et al. 2011). Our analysis has examined projected changes in the annual cycle of precipitation in monsoon regions, using a moist static energy framework to evaluate competing mechanisms, which have been previously identified as being important in precipitation changes over land.

The two mechanisms can be described as a *local* mechanism wherein enhanced evaporation leads to increased low level moist static energy and decreased stability with consequent increases in precipitation as well as recycling of moisture, and a *remote* mechanism in which a warmer tropical troposphere results in increased stability, and decreased precipitation. These are evaluated in time through the annual cycle, with an emphasis on the transition from dry to wet seasons. Also examined are relevant terms in the moisture budget (moisture flux divergence and evaporation). The *remote* (top down) mechanism controls the projected changes during winter and the *local* (bottom up) mechanism controls during summer in all monsoon regions. However, during the spring/early summer transition, reductions in boundary layer moisture availability due to decreases in evaporation and moisture convergence result in an enhanced convective barrier during early summer.

Our results indicate an early summer drying and late summer increase in rainfall in the American and African monsoons. This response is seen in the individual model results as well as the ensemble mean. In South and Southeast Asia, the precipitation changes do not show early summer drying, which appears to be due to abundant evaporation (and moisture availability) through the dry season. This suggests that evaporation can play an important role in the transition season: where moisture is available for evaporation, the local mechanism is activated and there is no reduction in early summer rainfall. Where there is insufficient moisture for local evaporation to initiate the local mechanism, early summer rainfall is shown to decrease. In all cases, once additional moisture is brought into the region via transport and convergence, rainfall increases compared to present due to increased atmospheric humidity resulting from warmer temperatures.

Analysis of idealized CMIP5 experiments which include only greenhouse gas forcing suggest that reductions in the early summer drying responses in Southeast Asia and West Africa are due to additional factors in the RCP8.5 scenario (i.e., the non-greenhouse gas forcings which include reductions in a number of aerosol species).

A number of caveats must be considered in the interpretation of these results. First, while there is more model agreement in these changes in these annual cycle changes than in annual or warm season means, it is clear that the models continue to exhibit substantial biases in tropical precipitation and in the annual cycle of rainfall in monsoon regions. In addition, the responses in several monsoon regions have been modified due to additional factors in the RCP8.5 scenario compared with CMIP3 SRES A2 results. Furthermore, while these results can help to explain the mechanisms which underlie projected precipitation changes over land-based monsoon regions, clearly these changes are embedded in large scale circulation response which is important over oceans. Thus, the global drivers of these changes over land may well be oceanic (amplification of SST annual cycle in the tropics, Dwyer et al. (2012)), and there may also be some influence on the northern margins of the subtropics related to poleward shifts in mid-latitude storm tracks (Scheff and Frierson 2012a,b).

Nevertheless, there are important implications of these results. First, annual or warm season averages will mask the coherent signals shown here in the CMIP5 projected annual cycle of rainfall. Second, the projected changes in the annual cycle of rainfall appear to be a response to greenhouse gas forcing. And third, the role of local evaporation and boundary layer moisture in the land-based monsoon regions is critical in determining the regional transition season response. Fasullo (2012) has also made this argument in a CMIP3 analysis of the global monsoon. Changes in the global monsoon precipitation have been difficult to evaluate both in observations and projections. As described in our results, viewing monsoons from their inherent ties to the annual cycle could help to fingerprint changes as they evolve.

Acknowledgments.

We acknowledge the World Climate Research Programme's Working Group on Coupled Modelling, which is responsible for CMIP, and we thank the climate modeling groups (listed in Table 1 of this paper) for producing and making available their model output. For CMIP the U.S. Department of Energy's Program for Climate Model Diagnosis and Intercomparison provides coordinating support and led development of software infrastructure in partnership with the Global Organization for Earth System Science Portals. This research was funded in part by the Climate Program Office at NOAA Model Analysis and Prediction Program (MAPP) #Award NA11OAR4310109. SR acknowledges the support of the DOE through the LANL LDRD program.

REFERENCES

Annamalai, H., K. Hamilton, and K. R. Sperber, 2007: The South Asian summer monsoon and its relationship with ENSO in the IPCC AR4 simulations. *Journal of Climate*, **20 (6)**, 1071–1092, URL `http://journals.ametsoc.org/doi/abs/10.1175/JCLI4035.1`.

Biasutti, M. and A. H. Sobel, 2009: Delayed Sahel rainfall and global seasonal cycle in a warmer climate. *Geophys. Res. Lett.*, **36**, doi:10.1029/2009GL041 303, URL `http://dx.doi.org/10.1029/2009GL041303`.

Biasutti, M., A. H. Sobel, and S. J. Camargo, 2009: The role of the Sahara low in summertime Sahel rainfall variability and change in the CMIP3 models. *Journal of Climate*, **22 (21)**, 5755–5771, URL `http://dx.doi.org/10.1175%2F2009JCLI2969.1`.

Chao, W. C. and B. Chen, 2001: The origin of monsoons. *Journal of the Atmospheric Sciences*, **58 (22)**, 3497–3507.

Chiang, J. C. and A. H. Sobel, 2002: Tropical tropospheric temperature variations caused by ENSO and their influence on the remote tropical climate. *J. Climate*, **15**, 2616–2631.

Chou, C. and J. D. Neelin, 2004: Mechanisms of global warming impacts on regional tropical precipitation. *J. Clim.*, **17**, 2688–2701.

Chou, C., J. D. Neelin, and H. Su, 2001: Ocean-atmosphere-land feedbacks in an idealized monsoon. *Quart. J. Roy. Meteor. Soc.*, **127**, 1869–1891.

Christensen, J. H., et al., 2007: Regional climate projections. *Climate Change 2007: The Physical Science Basis. Contribution of Working Group I to the Fourth Assessment Report of the Intergovernmental Panel on Climate Change*, S. Solomon, D. Qin, M. Manning,

Z. Chen, M. Marquis, K. Averyt, M. Tignor, and H. Miller, Eds., Cambridge University Press, New York, chap. 11, 235–336.

Collini, E. A., E. H. Berbery, V. R. Barros, and M. E. Pyle, 2008: How does soil moisture influence the early stages of the South American monsoon? *Journal of Climate*, **21 (2)**, 195–213, URL `http://dx.doi.org/10.1175%2F2007JCLI1846.1`.

Douville, H., J.-F. Royer, J. Polcher, P. Cox, N. Gedney, D. B. Stephenson, and P. J. Valdes, 2000: Impact of CO2 doubling on the Asian summer monsoon: Robust versus model-dependent responses. *J. Meteor. Soc. Japan*, **78**, 421–439.

Dwyer, J. G., M. Biasutti, and A. H. Sobel, 2012: Projected changes in the seasonal cycle of surface temperature. *Journal of Climate*, **25**, 6359–6374.

Fasullo, J., 2012: A mechanism for land–ocean contrasts in global monsoon trends in a warming climate. *Climate Dynamics*, **39 (5)**, 1137–1147, doi:10.1007/s00382-011-1270-3, URL `http://dx.doi.org/10.1007/s00382-011-1270-3`.

Giannini, A., 2010: Mechanisms of climate change in the semiarid African Sahel: The local view. *Journal of Climate*, **23 (3)**, 743–756, URL `http://dx.doi.org/10.1175%2F2009JCLI3123.1`.

Giannini, A., M. Biasutti, I. Held, and A. Sobel, 2008: A global perspective on African climate. *Climatic Change*, **90 (4)**, 359–383, URL `http://dx.doi.org/10.1007/s10584-008-9396-y`.

Grimm, A. M., J. S. Pal, and F. Giorgi, 2007: Connection between spring conditions and peak summer monsoon rainfall in south america: Role of soil moisture, surface temperature, and topography in eastern brazil. *Journal of Climate*, **20 (24)**, 5929–5945, URL `http://journals.ametsoc.org/doi/abs/10.1175/2007JCLI1684.1`.

Held, I. M., 2001: The partitioning of the poleward energy transport between the tropical ocean and atmosphere. *J. Atmos. Sci.*, **58**, 943–948.

Held, I. M. and B. J. Soden, 2006: Robust responses of the hydrological cycle to global warming. *J. Climate*, **19**, 5686–5699.

Lamarque, J.-F., G. Kyle, M. Meinshausen, K. Riahi, S. Smith, D. van Vuuren, A. Conley, and F. Vitt, 2011: Global and regional evolution of short-lived radiatively-active gases and aerosols in the representative concentration pathways. *Climatic Change*, **109 (1)**, 191–212, doi:10.1007/s10584-011-0155-0, URL `http://dx.doi.org/10.1007/s10584-011-0155-0`.

Lau, K., M. Kim, and K. Kim, 2006: Asian summer monsoon anomalies induced by aerosol direct forcing: the role of the Tibetan Plateau. *Climate Dynamics*, **26 (7)**, 855–864, URL `http://dx.doi.org/10.1007/s00382-006-0114-z`.

Li, W. and R. Fu, 2004: Transition of the large-scale atmospheric and land surface conditions from the dry to the wet season over Amazonia as diagnosed by the ECMWF reanalysis. *Journal of Climate*, **17 (13)**, 2637–2651, URL `http://dx.doi.org/10.1175%2F1520-0442%282004%29017%3C2637%3ATOTLAA%3E2.0.CO%3B2`.

Meehl, G., et al., 2007: *Climate Change 2007: The Physical Science Basis. Contribution of Working Group I to the Fourth Assessment Report of the Intergovernmental Panel on Climate Change*, chap. Global Climate Projections. Cambridge University Press, Cambridge, United Kingdom and New York, NY, USA.

Meehl, G. A., J. M. Arblaster, and W. D. Collins, 2008: Effects of black carbon aerosols on the Indian monsoon. *Journal of Climate*, **21 (12)**, 2869–2882, URL `http://journals.ametsoc.org/doi/abs/10.1175/2007JCLI1777.1`.

Neelin, J. D., C. Chou, and H. Su, 2003: Tropical drought regions in global warming and

El Niño teleconnections. *Geophys. Res. Lett.*, **30**, URL http://dx.doi.org/10.1029/2003GL018625.

Neelin, J. D. and I. M. Held, 1987: Modeling tropical convergence based on the moist static energy budget. *Mon. Wea. Rev.*, **115**, 3–12.

Rogelj, J., M. Meinshausen, and R. Knutti, 2012: Global warming under old and new scenarios using IPCC climate sensitivity range estimates. *Nature Clim. Change*, **(DOI: 10.1038/NCLIMATE1385)**.

Scheff, J. and D. Frierson, 2012a: Twenty-first-century multimodel subtropical precipitation declines are mostly midlatitude shifts. *Journal of Climate*, **25**, 4330–4347.

Scheff, J. and D. M. W. Frierson, 2012b: Robust future precipitation declines in CMIP5 largely reflect the poleward expansion of model subtropical dry zones. *Geophys. Res. Lett.*, **39 (18)**, doi:10.1029/2012GL052910, URL http://dx.doi.org/10.1029/2012GL052910.

Seager, R., et al., 2007: Model projections of an imminent transition to a more arid climate in southwestern North America. *Science*, **316 (5828)**, 1181–1184, URL http://www.sciencemag.org/cgi/content/abstract/316/5828/1181.

Seth, A., S. Rauscher, M. Rojas, A. Giannini, and S. Camargo, 2011: Enhanced spring convective barrier for monsoons in a warmer world? *Climatic Change*, **104 (2)**, 403–414, URL http://dx.doi.org/10.1007/s10584-010-9973-8.

Seth, A., M. Rojas, and S. A. Rauscher, 2009: CMIP3 projected changes in the annual cycle of the South American monsoon. *Climatic Change*, dOI 10.1007/s10584-009-9736-6.

Small, E. E., 2001: The influence of soil moisture anomalies on variability of the North American monsoon system. *Geophys. Res. Lett.*, **28 (1)**, 139–142, doi:10.1029/2000GL011652, URL http://dx.doi.org/10.1029/2000GL011652.

Sobel, A. H. and S. J. Camargo, 2010: Projected future seasonal changes in tropical summer climate. *Journal of Climate*, **24 (2)**, 473–487, doi:10.1175/2010JCLI3748.1, URL `http://dx.doi.org/10.1175/2010JCLI3748.1`.

Sobel, A. H., I. M. Held, and C. S. Bretherton, 2002: The ENSO signal in tropical tropospheric temperature. *Journal of Climate*, **15 (18)**, 2702–2706, URL `http://dx.doi.org/10.1175%2F1520-0442%282002%29015%3C2702%3AATESITT%3E2.0.CO%3B2`.

Sutton, R. T., B. Dong, and J. M. Gregory, 2007: Land/sea warming ratio in response to climate change: IPCC AR4 model results and comparison with observations. *Geophys. Res. Lett.*, **34 (L02701)**, doi:10.1029/2006GL028 164.

Tan, P.-H., C. Chou, and J.-Y. Tu, 2008: Mechanisms of global warming impacts on robustness of tropical precipitation asymmetry. *Journal of Climate*, **21**, 5585–5602.

Tanaka, H. L., N. Ishizaki, and D. Nohara, 2005: Intercomparison of the intensities and trends of Hadley, Walker and monsoon circulations in the global warming projections. *SOLA*, **1**, 77–80, doi:doi:10.2151/sola.2005021.

Taylor, C. M., P. P. Harris, and D. J. Parker, 2010: Impact of soil moisture on the development of a Sahelian mesoscale convective system: A case-study from the AMMA special observing period. *Quarterly Journal of the Royal Meteorological Society*, **136 (S1)**, 456–470, URL `http://dx.doi.org/10.1002/qj.465`.

Taylor, K. E., R. J. Stouffer, and G. A. Meehl, 2011: An overview of CMIP5 and the experiment design. *Bulletin of the American Meteorological Society*, **93 (4)**, 485–498, doi:10.1175/BAMS-D-11-00094.1, URL `http://dx.doi.org/10.1175/BAMS-D-11-00094.1`.

Trenberth, K. E., D. P. Stepaniak, and J. M. Caron, 2000: The global monsoon as seen through the divergent atmospheric circulation. *Journal of Climate*, **13 (22)**, 3969–3993, URL `http://journals.ametsoc.org/doi/abs/10.1175/1520-0442%282000%29013%3C3969%3ATGMAST%3E2.0.CO%3B2`.

Turner, A. G. and H. Annamalai, 2012: Climate change and the South Asian summer monsoon. *Nature Clim. Change*, **2 (8)**, 587–595, URL http://dx.doi.org/10.1038/nclimate1495.

van Vuuren, D., et al., 2011: The Representative Concentration Pathways: An overview. *Climatic Change*, **109 (1)**, 5–31, doi:10.1007/s10584-011-0148-z, URL http://dx.doi.org/10.1007/s10584-011-0148-z.

Vecchi, G. A. and B. J. Soden, 2007: Global warming and the weakening of the tropical circulation. *J. Climate*, **20**, 4316–4340.

Vera, C., G. Silvestri, B. Liebmann, and P. Gonzalez, 2006: Climate change scenarios for seasonal precipitation in South America from IPCC-AR4 models. *Geophys. Res. Let.*, **33**, doi:10.1029/2006GL025759.

Villarini, G. and G. A. Vecchi, 2012: Twenty-first-century projections of North Atlantic tropical storms from CMIP5 models. *Nature Clim. Change*, **2 (8)**, 604–607, URL http://dx.doi.org/10.1038/nclimate1530.

Wang, B. and Q. Ding, 2006: Changes in global monsoon precipitation over the past 56 years. *Geophys. Res. Lett.*, **33 (6)**, URL http://dx.doi.org/10.1029/2005GL025347.

Wang, B., J. Liu, H.-J. Kim, P. Webster, and S.-Y. Yim, 2012: Recent change of the global monsoon precipitation (1979–2008). *Climate Dynamics*, **39 (5)**, 1123–1135, doi:10.1007/s00382-011-1266-z, URL http://dx.doi.org/10.1007/s00382-011-1266-z.

Webster, P. J., V. O. Magaña, T. N. Palmer, J. Shukla, R. A. Thomas, M. Yanai, and T. Yasunari, 1998: Monsoons: Processes, predictability, and the prospects for prediction. *J. Geophys. Res.*, **103**, 14 451–14 510, doi:10.1029/97JC02719.

Xie, P. and P. Arkin, 1996: Analysis of global monthly precipitation using gauge observation, satellite estimates and numerical model predictions. *J. Climate*, **9**, 840–858.

List of Tables

Table 1. CMIP5 coupled models analyzed in this study using the Historical and RCP8.5 experiments. Stars indicate models for which Pre-industrial Control and 1%CO2 experiments are employed. Atmosphere resolution is shown as the number of grids in latitude and longitude, respectively.

Modeling Center	Model	Realization	Atm Resolution
NCAR	CCSM4	r1i1p1	192 x 288
CNRM-CERFACS	CNRM-CM5	r2i1p1	128 x 256
CSIRO-BOM	CSIRO-Mk3-6*	r1i1p1	96 x 192
CCCMA	CanESM2*	r1i1p1	64 x 128
FIO	FIO-ESM	r1i1p1	64 x 128
NOAA GFDL	GFDL-CM3	r1i1p1	90 x 144
	GFDL-ESM2M*	r1i1p1	90 x 144
NASA GISS	GISS-E2-R	r1i1p1	90 x 144
MOHC	HadGEM2*	r1i1p1	144 x 192
IPSL	IPSL-CM5A-LR*	r1i1p1	96 x 96
	IPSL-CM5A-MR*	r1i1p1	143 x 144
MIROC	MIROC-ESM*	r1i1p1	64 x 128
	MIROC5*	r1i1p1	128 x 256
MPI-M	MPI-ESM-LR*	r1i1p1	96 x 192
MRI	MRI-CGCM3	r1i1p1	160 x 320
NCC	NorESM1*	r1i1p1	96 x 144
INM	INM-CM4*	r1i1p1	120 x 180

List of Figures

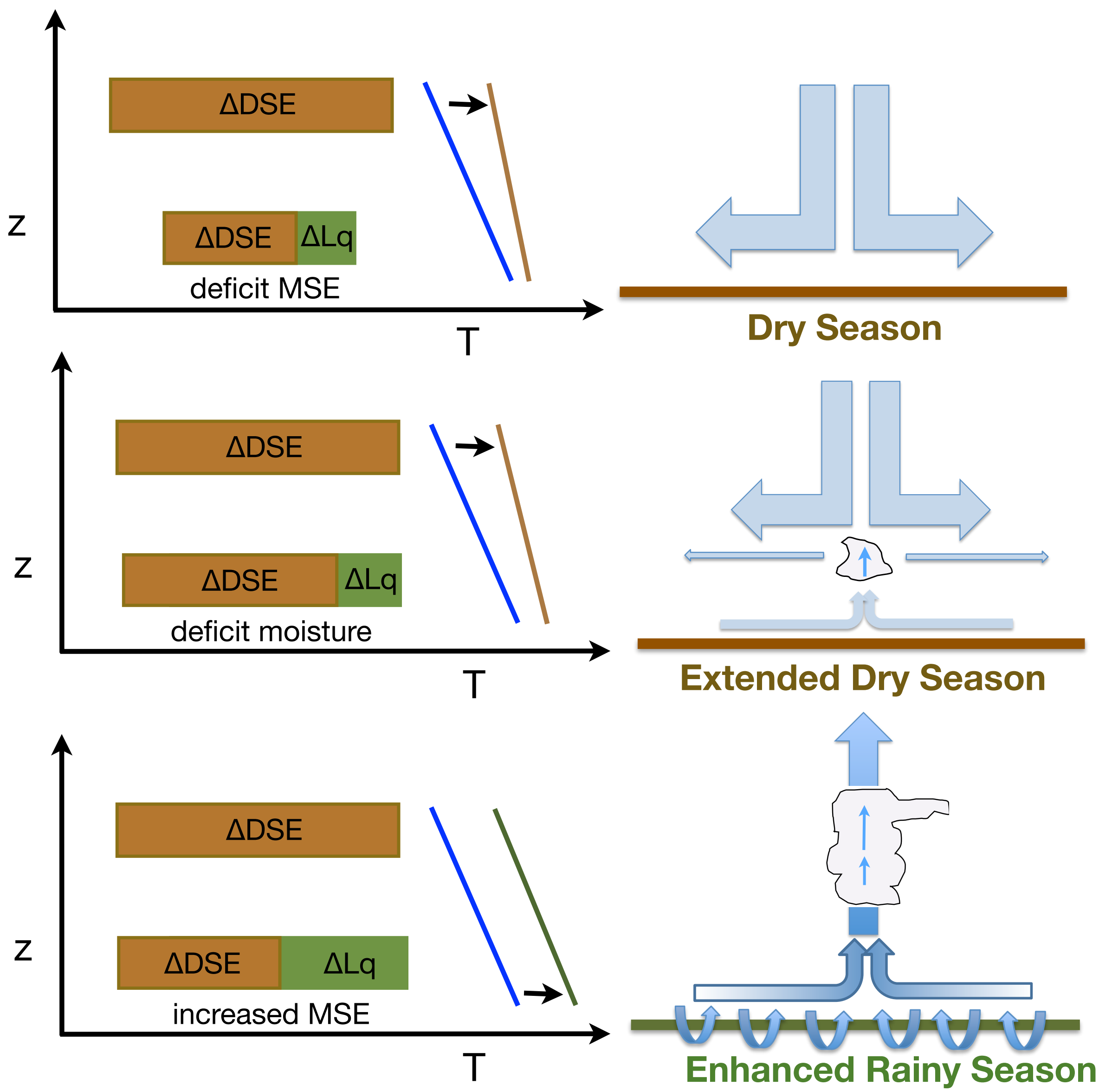

FIG. 1. Schematic of remote and local mechanisms as described in the text.

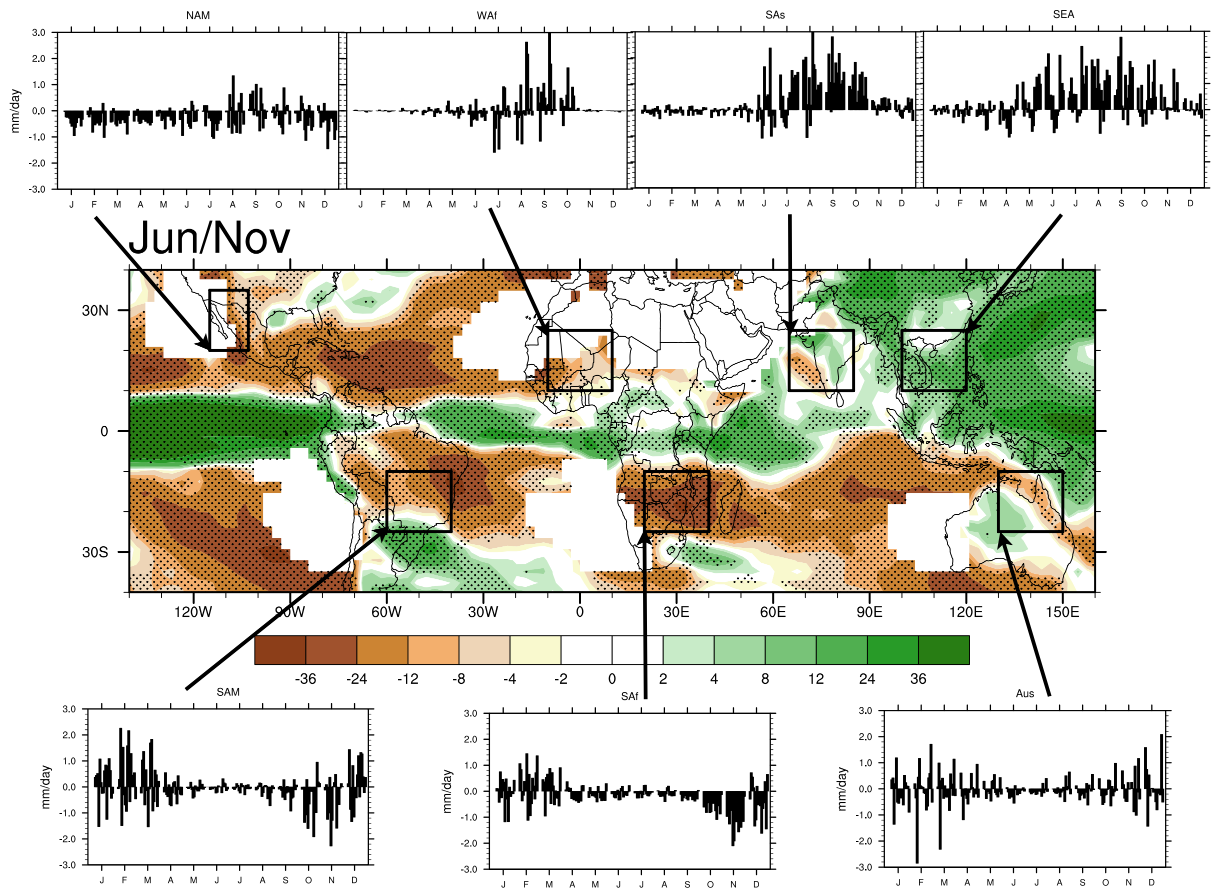

Fig. 2. Precipitation percent difference (colors) between the 17-model ensemble mean RCP8.5 minus Hist, masked for areas where climatological precipitation is less than .5 mm/day. Map shows June for northern and November for southern hemispheres. Stippling indicates significance at the 1% level. Individual model monthly precipitation differences (mm/day, RCP8.5 - Hist) are given in bar charts for each region as specified in the map.

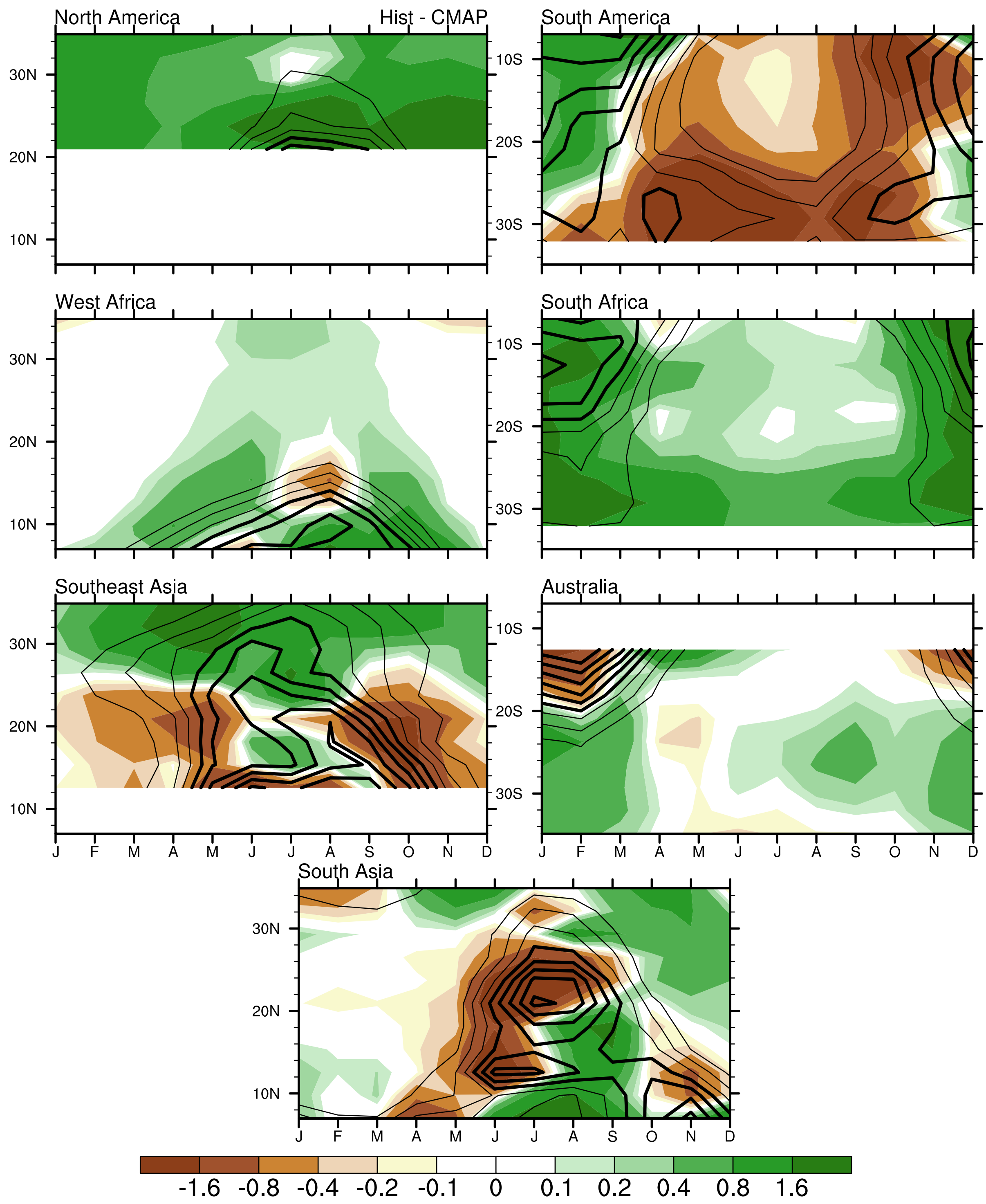

FIG. 3. Annual cycles of regional monsoon precipitation, averaged for longitudes as specified in text, from CMAP observed estimate (black contours, 2 - 10 with interval 1, thicker lines begin at 5 mm/day) and differences between the CMIP5 17-model ensemble mean Hist minus CMAP (colors, mm/day) for the period 1981-2005.

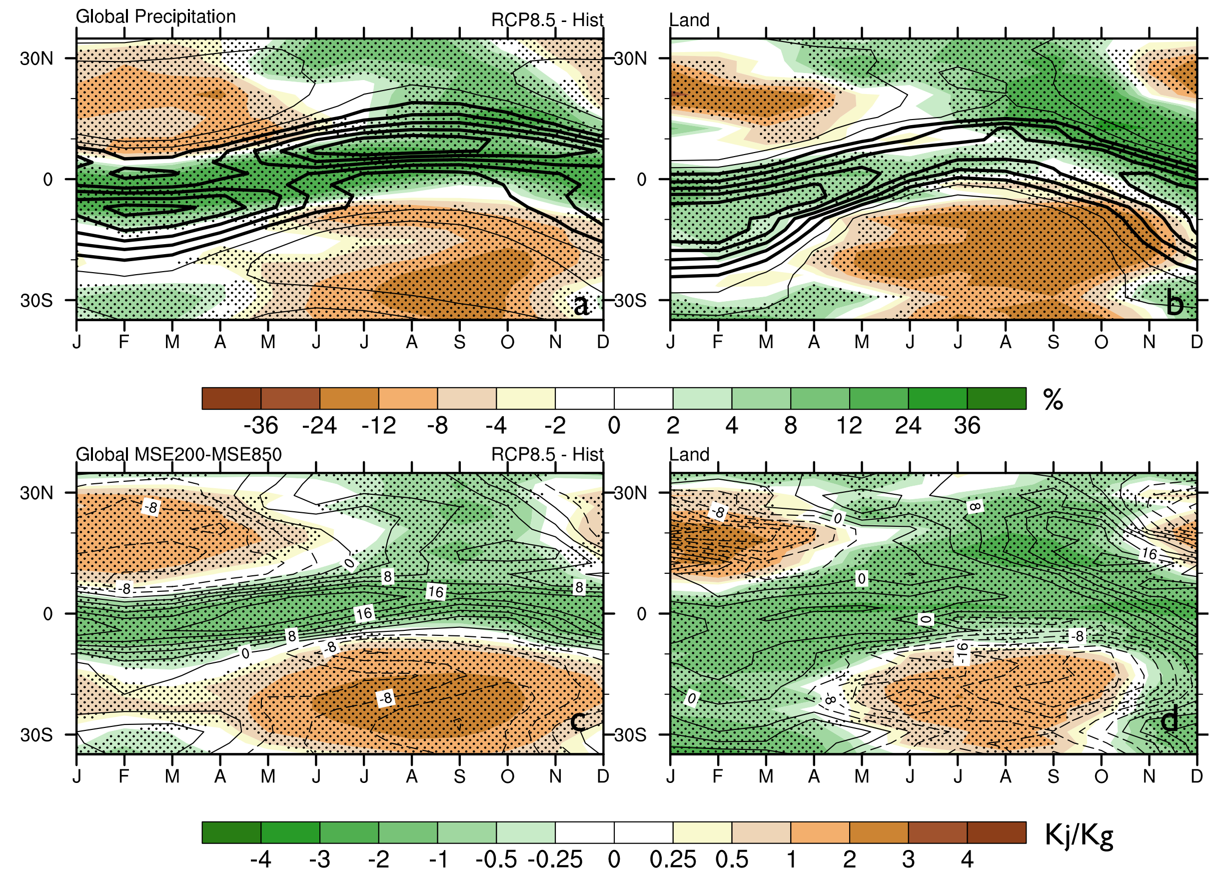

FIG. 4. Annual cycles of global tropical precipitation (a,b) and $vMSE$ (c,d), averaged for all longitudes (a,c) and for land only (b,d) for 17-model ensemble mean Hist (black contours) and RCP8.5 minus Hist (colors). Stippling indicates significance at the 1% level.

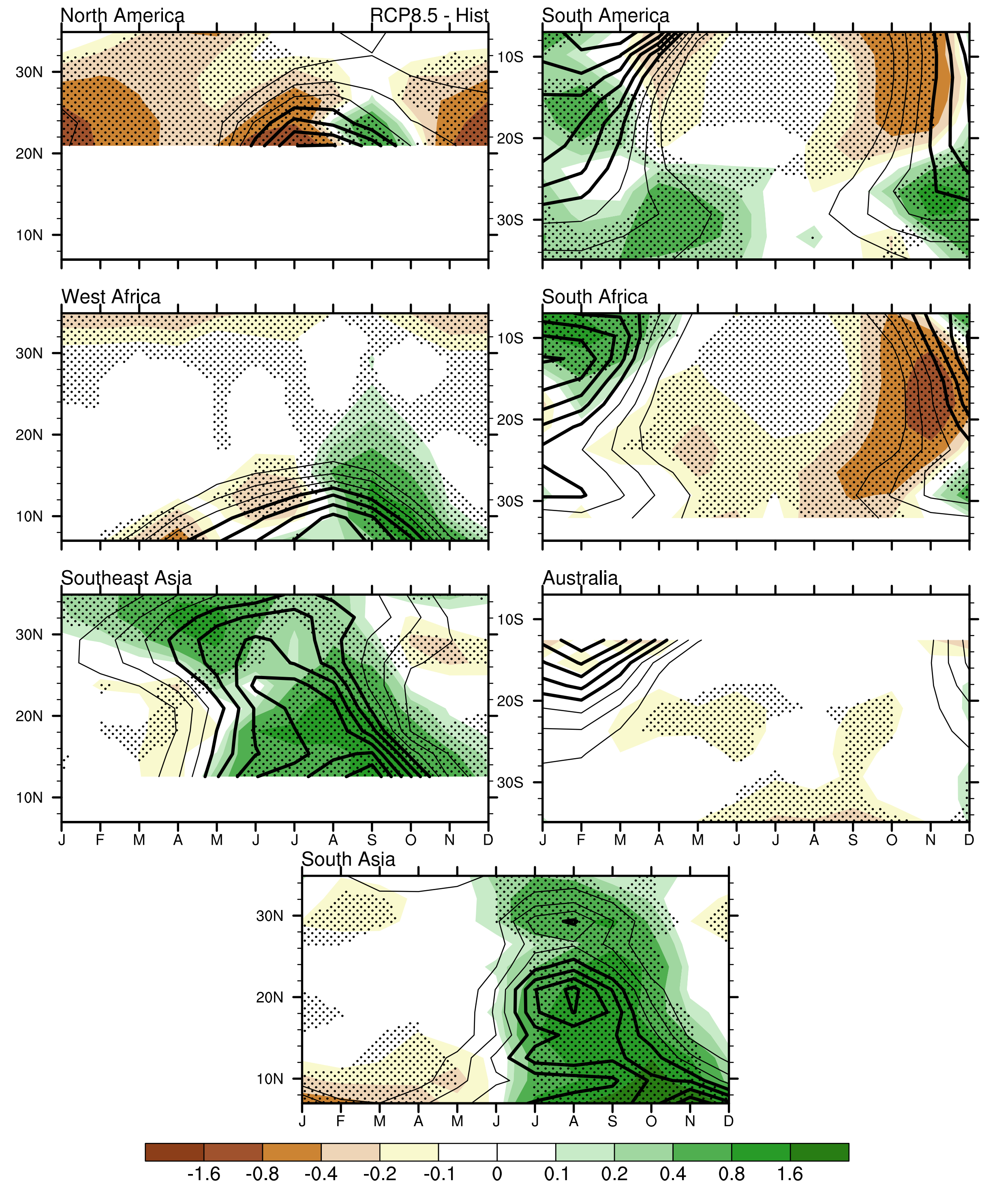

FIG. 5. Zonal mean annual cycles of precipitation (mm/day), averaged for longitudes for each monsoon region as specified in the text for the 17-Model ensemble mean Hist (black contours) and projected changes, RCP8.5 minus Hist (colors). Climatology and differences are masked for land.

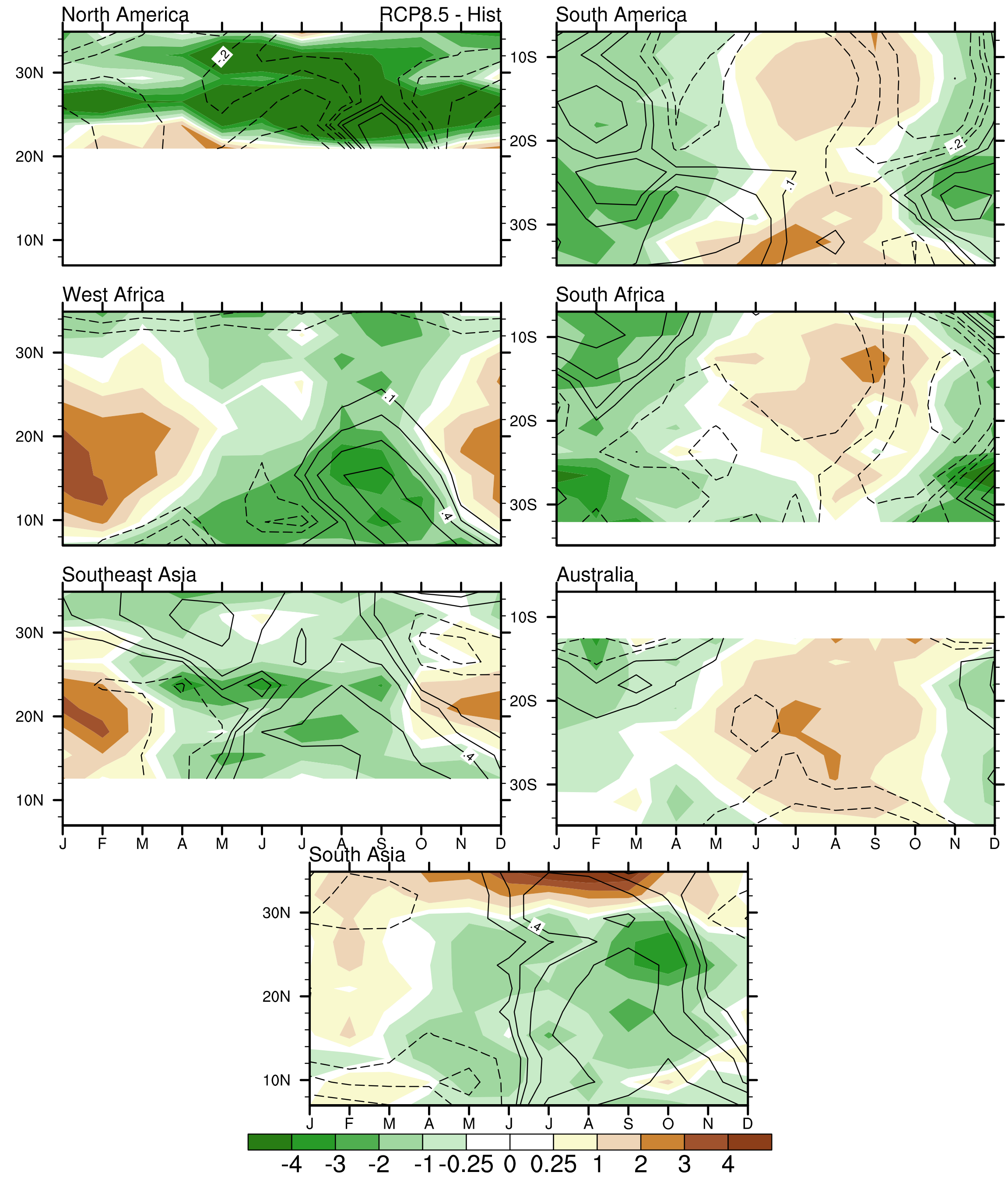

FIG. 6. As in Fig. 5 execpt for Moist Static Energy vertical difference (MSEv), with precipitation changes given in mm/day (black contours) for reference .

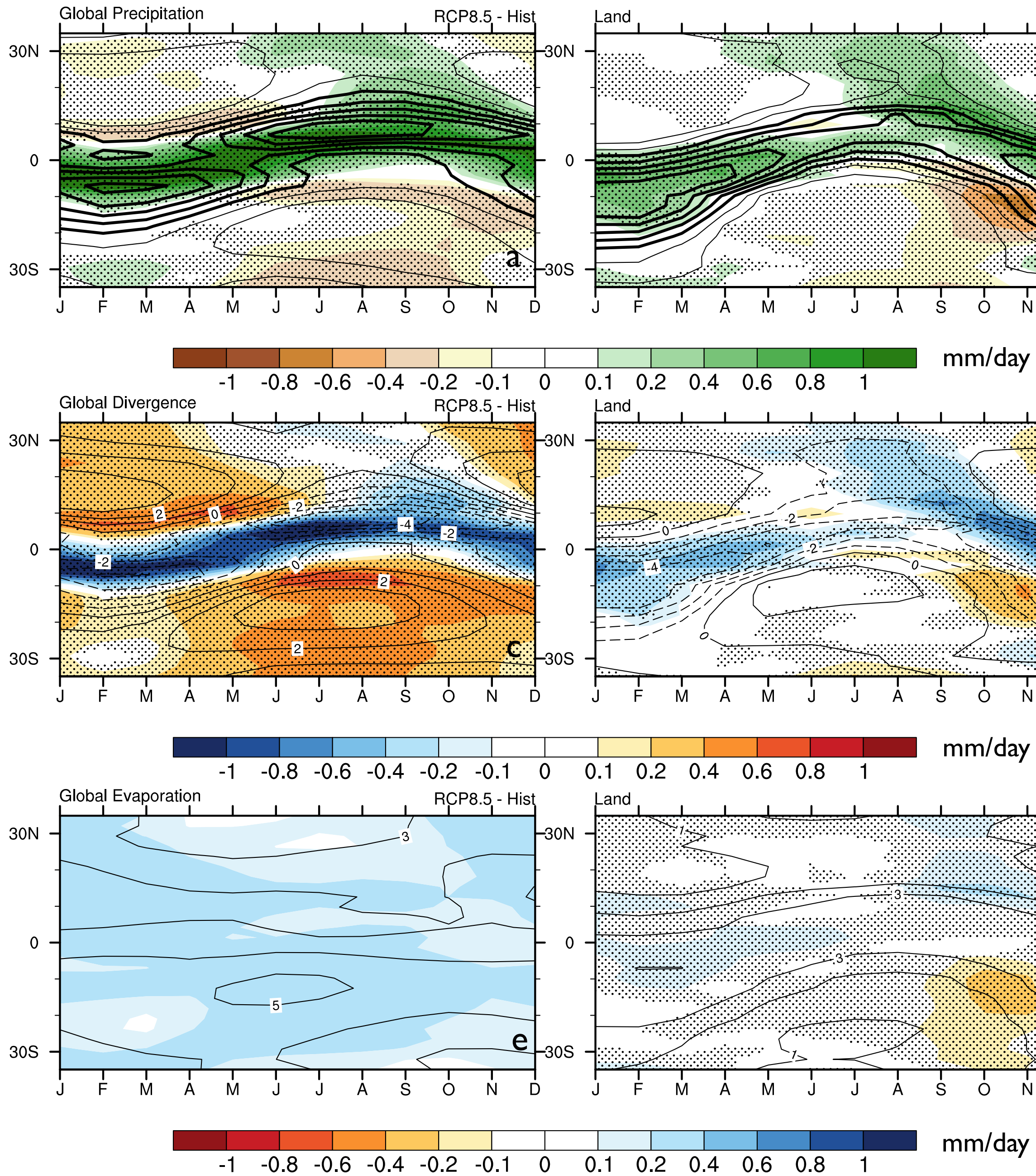

FIG. 7. Zonal mean annual cycles of global tropical Precipitation (a,b), Divergence (c,d), and Evaporation (e,f) (a,c,e) and for land only (b,d,f) for 17-model ensemble mean Hist (black contours) and RCP8.5 minus Hist (colors) with simulated Hist climatology (black contours), all in mm/day. Stippling indicates significance at the 1% level.

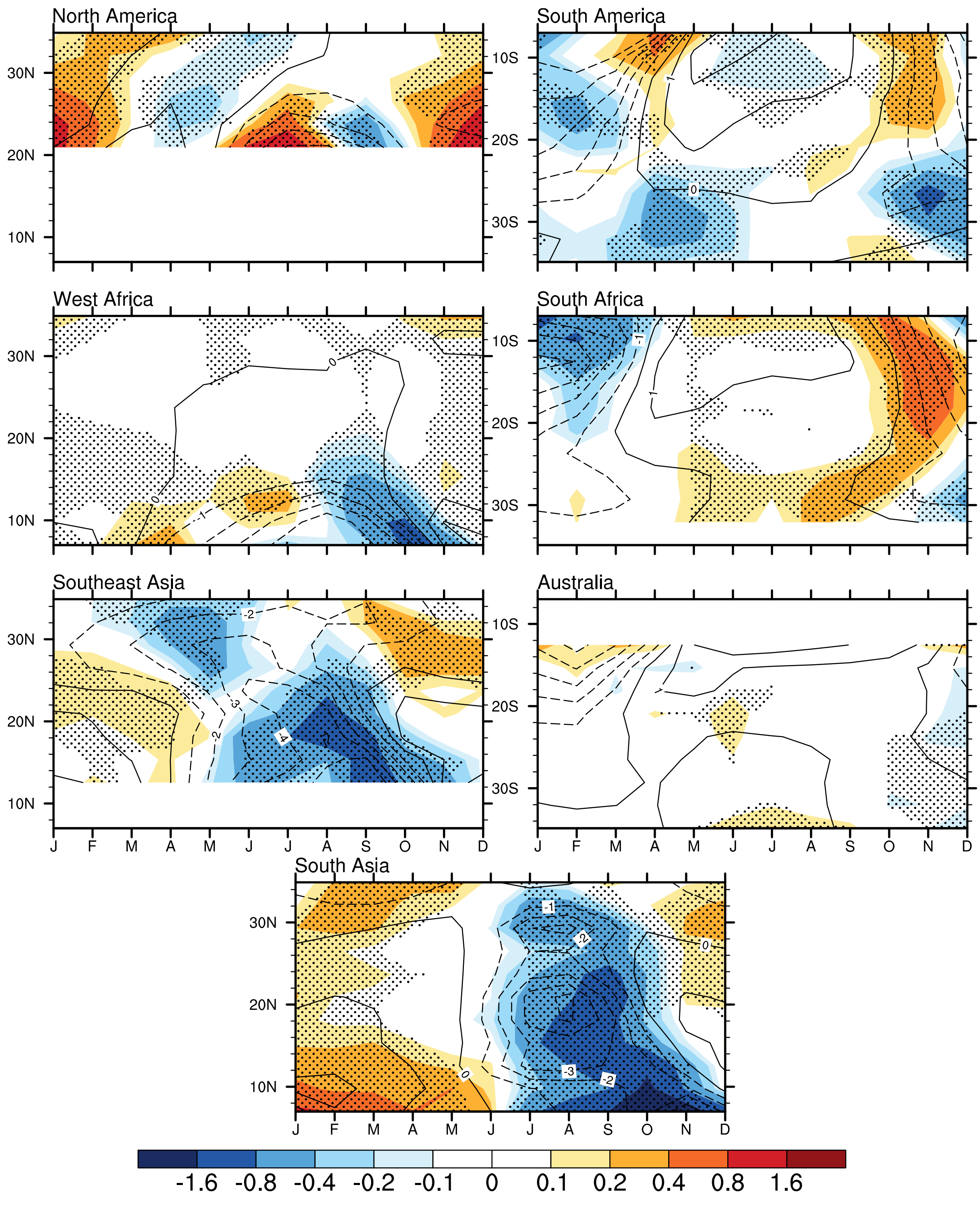

FIG. 8. As in Fig. 5 but for divergence.

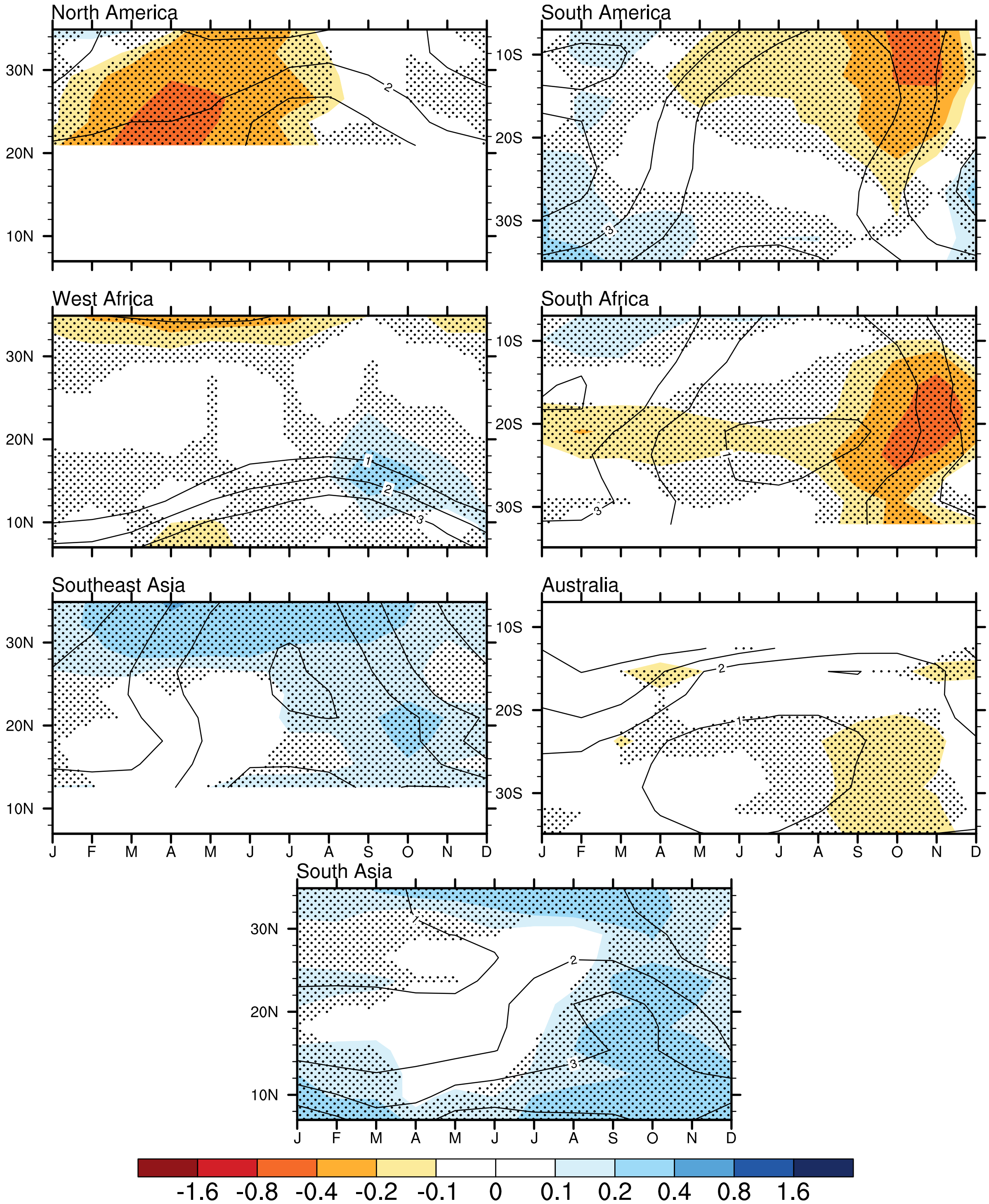

FIG. 9. As in Fig. 5 but for evaporation.

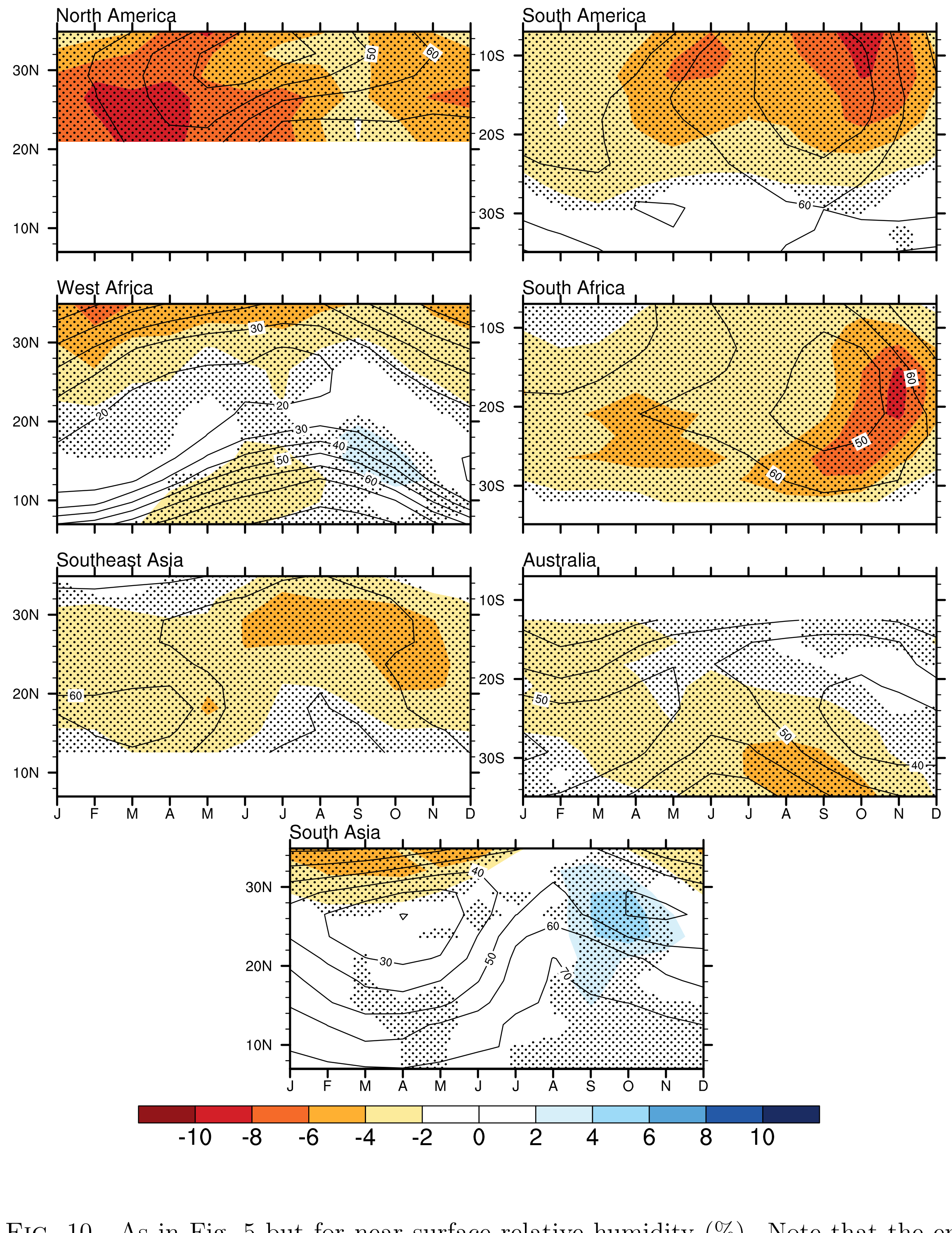

Fig. 10. As in Fig. 5 but for near surface relative humidity (%). Note that the ensemble mean for this variable is based on 14 models only, as it was not available for three models (FIO-ESM, GFDL-CM3, and MPI-ESM-LR) at the time of writing.

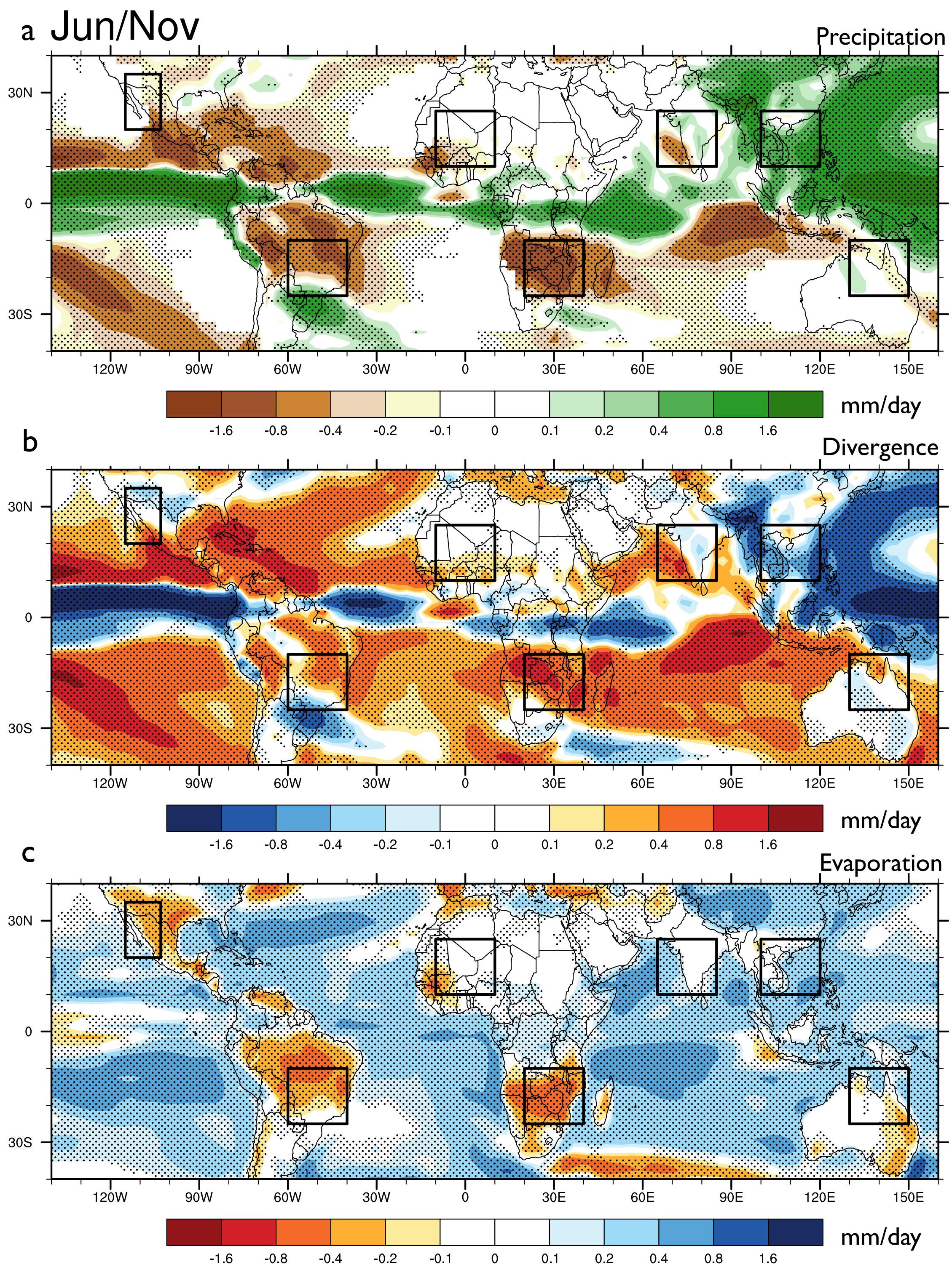

FIG. 11. Early summer: June (northern hemisphere) November (southern hemisphere) RCP8.5 minus Hist differences in Precipitation (a) Divergence (b), and Evaporation (c) in mm/day. Boxes specify monsoon regions. Stippling indicates significance.

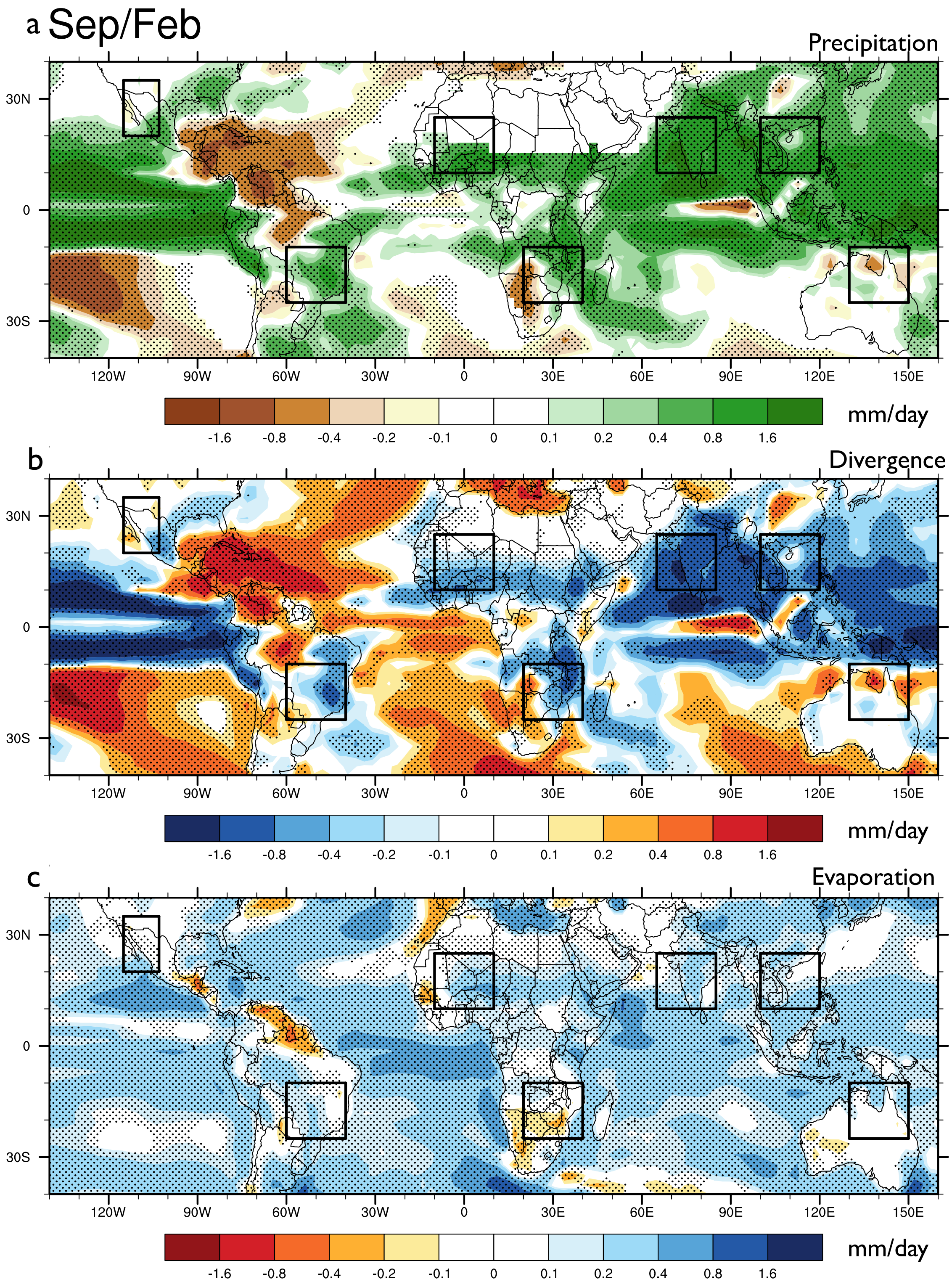

FIG. 12. As in Fig. 11 but for late summer, September/February.

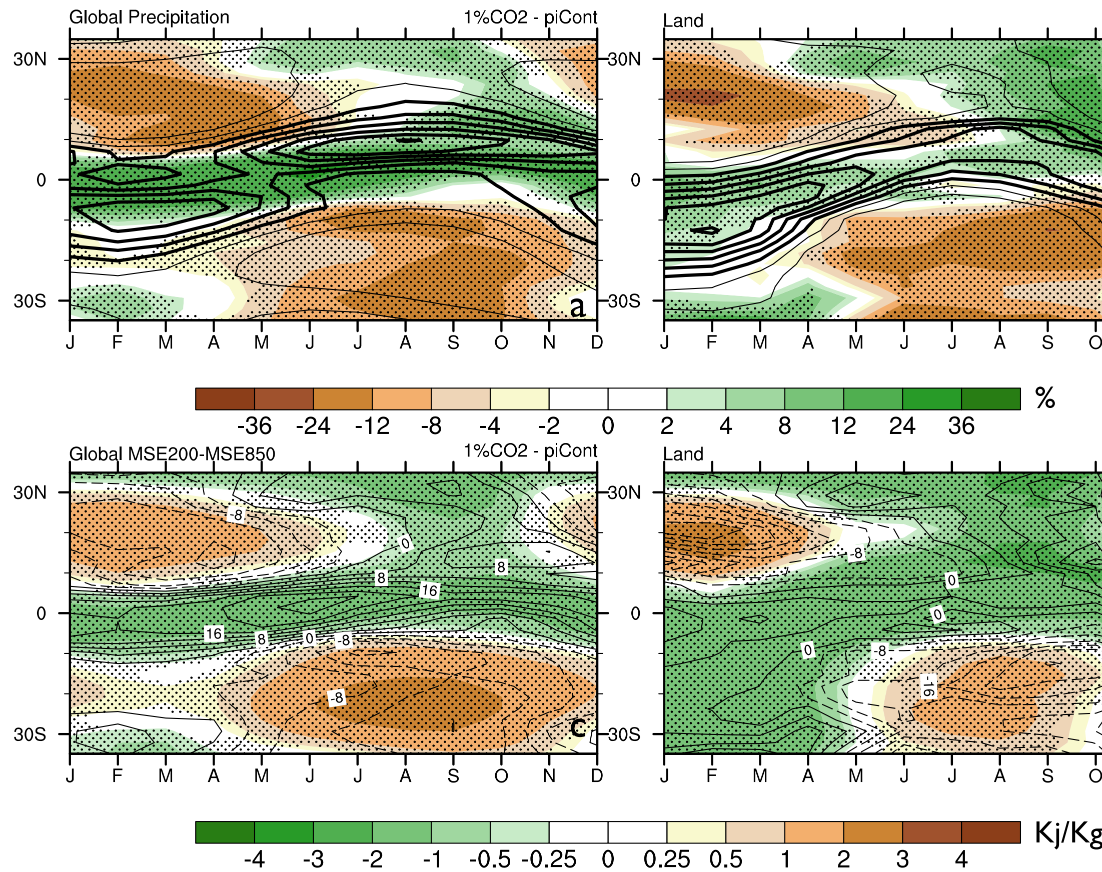

FIG. 13. As in Fig. 4 but for CMIP5 piCont (black lines) and differences 1%CO2 minus piCont (colors) for 11 models.

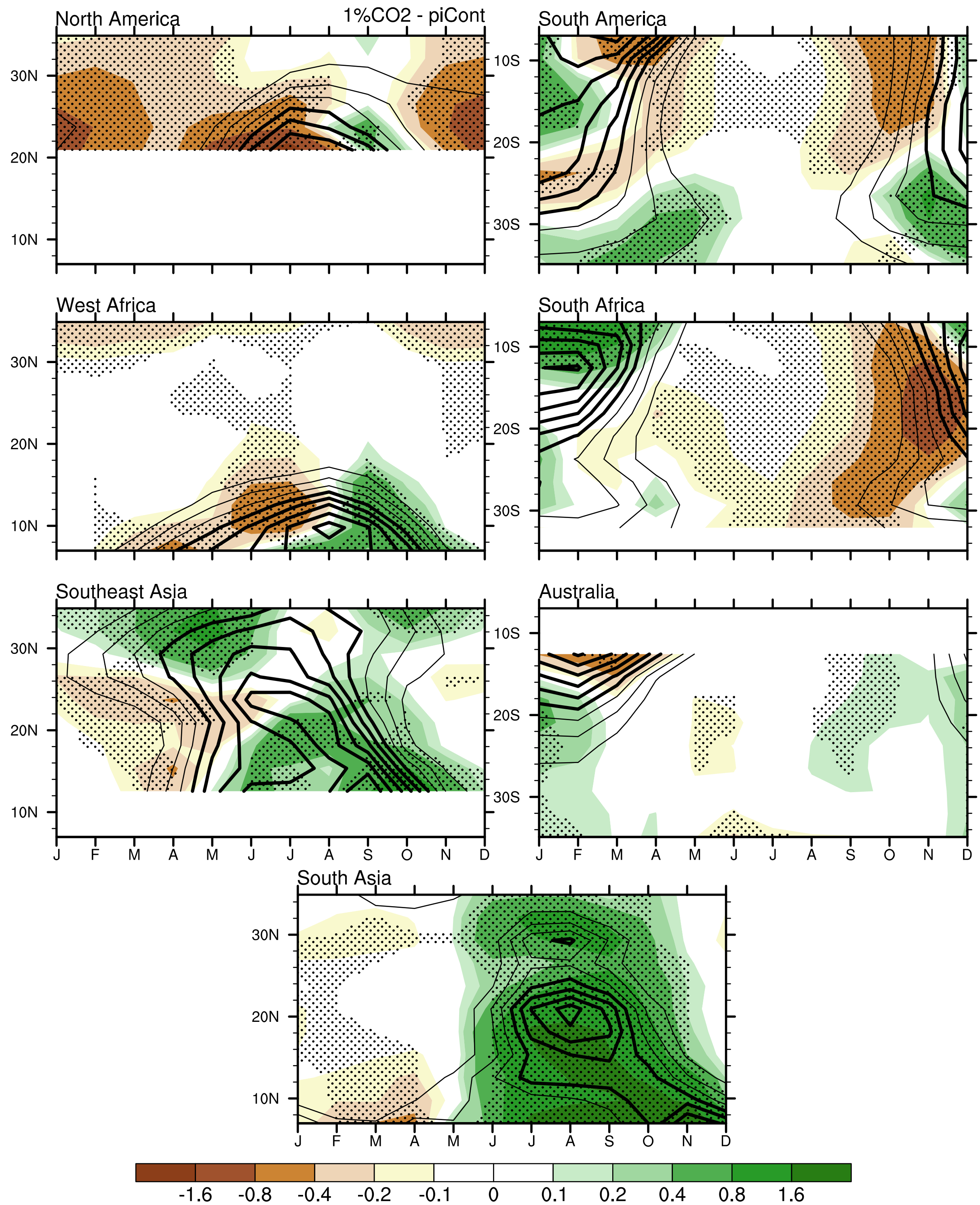

Fig. 14. As in Fig. 5 but for CMIP5 piCont (black lines) and differences 1%CO2 minus piCont (colors) for 11 models.